forests

MDPI

Article

The Dynamics of Transpiration to Evapotranspiration Ratio under Wet and Dry Canopy Conditions in a Humid Boreal Forest

Bram Hadiwijaya [1], Steeve Pepin [2], Pierre-Erik Isabelle [1,3] and and Daniel F. Nadeau [1,*]

[1] CentrEau—Water Research Center, Department of Water and Civil Engineering, Université Laval, 1065 avenue de la Médecine, Québec, QC G1V 0A6, Canada; bram.hadiwijaya.1@ulaval.ca (B.H.); pierre-erik.isabelle.1@ulaval.ca (P.-E.I.)

[2] Centre de Recherche et d'Innovation sur les Végétaux, Department of Soil and Agri-Food Engineering, Université Laval, 2480 boulevard Hochelaga, Québec, QC G1V 0A6, Canada; Steeve.Pepin@fsaa.ulaval.ca

[3] Premier Tech, 1 avenue Premier, Rivière-du-Loup, QC G5R 6C1, Canada

* Correspondence: daniel.nadeau@gci.ulaval.ca

Received: 31 January 2020; Accepted: 19 February 2020; Published: 21 February 2020

Abstract: Humid boreal forests are unique environments characterized by a cold climate, abundant precipitation, and high evapotranspiration. Transpiration (E_T), as a component of evapotranspiration (E), behaves differently under wet and dry canopy conditions, yet very few studies have focused on the dynamics of transpiration to evapotranspiration ratio (E_T/E) under transient canopy wetness states. This study presents field measurements of E_T/E at the Montmorency Forest, Québec, Canada: a balsam fir boreal forest that receives $\sim$ 1600 mm of precipitation annually (continental subarctic climate; Köppen classification subtype Dfc). Half-hourly observations of E and E_T were obtained over two growing seasons using eddy-covariance and sap flow (Granier's constant thermal dissipation) methods, respectively, under wet and dry canopy conditions. A series of calibration experiments were performed for sap flow, resulting in species-specific calibration coefficients that increased estimates of sap flux density by 34% $\pm$ 8%, compared to Granier's original coefficients. The uncertainties associated with the scaling of sap flow measurements to stand E_T, especially circumferential and spatial variations, were also quantified. From 30 wetting–drying events recorded during the measurement period in summer 2018, variations in E_T/E were analyzed under different stages of canopy wetness. A combination of low evaporative demand and the presence of water on the canopy from the rainfall led to small E_T/E. During two growing seasons, the average E_T/E ranged from 35% $\pm$ 2% to 47% $\pm$ 3%. The change in total precipitation was not the main driver of seasonal E_T/E variation, therefore it is important to analyze the impact of rainfall at half-hourly intervals.

Keywords: boreal forest; eddy-covariance; evapotranspiration; sap flow; transpiration; leaf wetness; interception

---

1. Introduction

Boreal forests occupy around a third of the world's forest biomes [1] and represent the second largest vegetated area behind tropical forests [2]. Given its large size, the boreal forest regulates water fluxes over a vast area and thus impacts global climatology and hydrology [3,4]. Understanding the interactions between this ecosystem and the atmosphere is crucial [3,5], as it is particularly vulnerable to climate change [6]. Among the anticipated changes, the boreal biome is expected to experience a large increase in temperatures [7,8] and a modest increase in precipitation [7]. Although evapotranspiration is more sensitive to changes in precipitation than temperature [9], a possible shift in the geographical distribution of conifer tree species due to climate change could alter the composition of boreal forests (e.g., more deciduous tree species) and result in greater evapotranspiration in the summertime [2].

Among the water exchanges between forest ecosystem and atmosphere, evapotranspiration (E) is certainly the least well characterized, making its study of utmost importance [10–12]. In forest ecosystems, E is the transfer of water to the atmosphere through the combination of (i) evaporation from the soil and understory surfaces evapotranspiration (E_G), as well as evaporation from wet overstory canopy surfaces (E_C), and (ii) vegetation transpiration (E_T) [13–15]. In this paper, E_T is defined as the overstory canopy transpiration. The ratio of transpiration to evapotranspiration (E_T/E) on a global scale depends on the leaf coverage over a given land surface and the growing stage of the forest stands [16]. Generally, E_T represents the largest fraction of total boreal forest E during the growing season [17], except in treed peatlands [18,19] and in dry sparse forests where E_G is a significant proportion of E [18]. Despite their importance, in situ measurements of E_T/E are rather minimal in boreal forests [17–19], especially in wet regions of the biome.

A recent study by Isabelle et al. [20] at a humid boreal forest in eastern Canada found the mean cumulative annual E to be $\approx$ 550 mm, the highest amongst a total of 15 sites across the boreal biome, despite representing a rather modest fraction of the mean annual precipitation ($\approx$ 1600 mm). In humid boreal forests, where tree growth and E_T rate are not limited by water availability, one may expect a relatively large E_T/E ratio. On the other hand, frequent precipitation implies a low vapor pressure deficit and reduced solar radiation, both not favoring E nor E_T [21,22]. Further, rain droplets covering the foliage have also been shown to be an important physical factor limiting E_T [22]. In brief, we still lack a proper understanding of the evolution of the E_T/E ratio in sites subjected to frequent variations in canopy wetness.

Another key issue relates to the dynamics of both E and E_T under different canopy wetness conditions. Nearly all of the studies on E_T/E of forests biomes reported to date have contrasted wet versus dry canopy conditions only [23–26], with the exception of Aparecido et al. [22], where the authors have investigated the variations of E_T under different canopy wetness (dry, semi-dry and wet) conditions. Yet the vertical distribution of leaf wetness within a forest canopy is a very important factor for simulating E_T, especially in models that use the single big leaf approach [13].

The most common method for estimating tree E_T is to measure water flux in sapwood, commonly referred to as sap flow [27–29]. Sap flow monitoring can quantify the whole-plant water use continuously, regardless of the species, canopy, and terrain heterogeneity [30–32]. On the basis of the SAPFLUXNET database, the thermal dissipation method [33,34] appears to be by far the most popular technique to measure sap flow [35]. This method monitors the temperature difference between two probes inserted in sapwood to quantify sap flux density (F_d) for a given sapwood depth and height [23,28]. Results can then be scaled up to the whole tree and extrapolated to obtain tree-stand E_T [24].

Caution should be taken when estimating sap flow with this approach, as multiple sources of uncertainty exist [36]. First, one should use species-specific calibration factors in the calculation of F_d [31,37,38]. Peters et al. [36] found that 90% of thermal dissipation sap flow studies use the calibration coefficients from the original experiment by Granier [33]. However, several studies have reported variability in the empirical coefficients across different tree species (e.g., [31,36,39]). Other uncertainties may arise from sensors being partially inserted into non-conducting heartwood [40], circumferential variations of F_d [41–43], raw signal processing to determine maximum temperature differences between two probes during zero flow [29,44], and the upscaling and extrapolation processes from sapwood scale to tree-stand scale [23,45].

If sap flow measurements are the norm to estimate E_T, the eddy-covariance method is the most direct and well-accepted approach to monitor total E over forest stands (e.g., [23,46,47]). It has been regularly paired with sap flow measurements to estimate E_T and E independently (e.g., [19,23,48]). Comparing the results from tree-based sap flow measurements with eddy-covariance, which has a much larger spatial scale (footprint area 10^4–10^6 m^2), can, however, be a challenge [49]. The heterogeneity between trees on which sap flow measurements are being conducted can lead to poor representation of the E_T rate within the eddy-covariance measurement footprint [50].

The main objective of this study is to assess the impact of high precipitation on the dynamics of E_T/E from half-hourly to seasonal time scales in a humid boreal forested site. In order to achieve this goal, we have two specific objectives. The first is to measure the E_T of balsam fir (*Abies balsamea* (L.) Mill.) trees, notably by calibrating Granier's approach for this tree species, and then by analyzing the multiple sources of uncertainty in the upscaling process. The second specific objective is to monitor the state of the canopy around rainfall events and link this to the dynamics of E and E_T.

2. Materials and Methods

2.1. Study Site

This study was conducted in a region representative of the humid boreal forest, namely Montmorency Forest in eastern Canada (47°17′18″ N; 71°10′05.4″ W) [20]. This region is under the influence of a continental subarctic climate with a short and cool growing season occurring between June and October [51]. The mean annual temperature and precipitation are 0.5°C and 1583 mm (61% rain, 39% snow), respectively [52]. The site is located within the balsam fir-white birch bioclimatic domain, the dominant vegetation being balsam fir (*Abies balsamea* (L.) Mill.) with sparse occurrences of white birch (*Betula papyrifera* Marsh), white spruce (*Picea glauca* (Moench) Voss) and black spruce (*Picea mariana* Mill.) [53,54].

The measurement sites were located around two eddy-covariance towers in an experimental watershed (Figure 1a) called the "Bassin Expérimental du Ruisseau des Eaux-Volées" (BEREV) [53–56]. The first tower is surrounded by a young tree stand that developed after an 85% clear cut that occurred in 1993–1994 [51], hence this stand is referred to as the "Juvenile" site (Figure 1b,c). The second tower is located 1.3 km east of the first tower and is surrounded by a younger stand resulting from logging that happened progressively between 2000 and 2010 and is designated as the "Sapling" site (Figure 1d,e). The age difference between trees in Juvenile and Sapling sites allowed us to investigate the dynamics of E_T/E in stands with different characteristics (Table 1). Specifically, the more mature trees at the Juvenile site were taller and had larger stem diameter and higher leaf area index compared to the younger trees of the Sapling site.

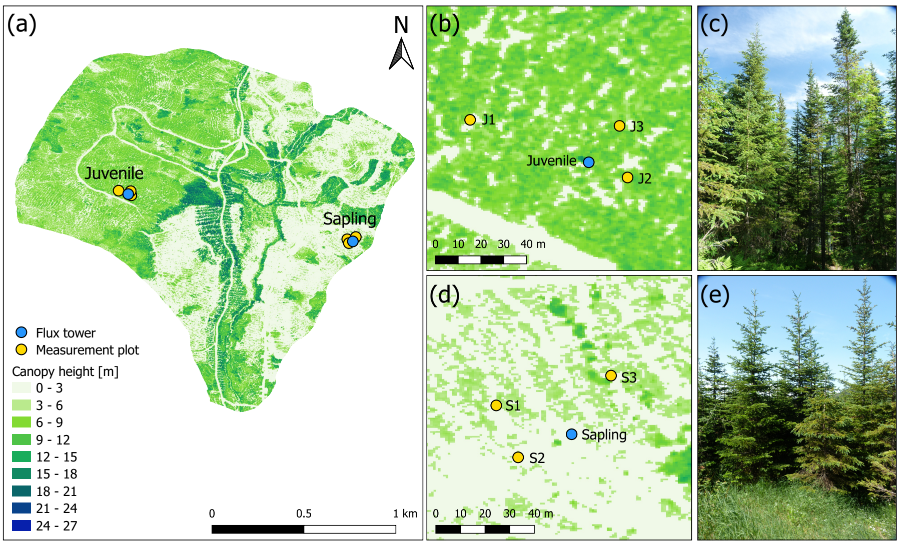

Figure 1. (**a**) Location of Juvenile and Sapling flux towers in the experimental watershed; (**b**) location of measurement plots around Juvenile flux tower; (**c**) trees at the Juvenile site; (**d**) location of measurement plots around Sapling flux tower; and (**e**) trees at the Sapling site. Vegetation heights are computed from LiDAR surveys (Source: Ministère des Forêts, de la Faune et des Parcs du Québec) collected in 2016.

Table 1. Characteristics of balsam fir trees inside the 400-m^2 plot: tree density per hectare (extrapolated from the number of trees in 0.04 ha), canopy height (h), diameter at breast height (DBH), leaf area index (LAI) and sapwood area per unit ground area (S_T). Values are mean ± standard deviation.

Plot	Tree Density [Number of Trees per ha]	h [m]	DBH [cm]	LAI [m^2 m^{-2}]	S_T [m^2 m^{-2}]
Juvenile					
J1	6500	10.2 ± 3.2	10.2 ± 2.5	3.87	0.00253
J2	5000	11.6 ± 3.5	11.4 ± 3.8	3.35	0.00252
J3	6750	9.5 ± 2.7	8.9 ± 2.0	3.55	0.00223
Sapling					
S1	9250	6.3 ± 1.2	6.8 ± 1.5	3.07	0.00157
S2	9250	5.6 ± 1.1	5.6 ± 1.2	2.96	0.00154
S3	6750	5.7 ± 1.5	4.6 ± 1.0	2.58	0.00147

Three 400-m^2 circular plots were established around each flux tower. The plot locations were determined based on the relative flux footprint contribution. The flux footprint area depends on the direction of prevailing winds. Canopy height and DBH were measured for every tree inside the plots, whereas the leaf area index was measured under overcast sky conditions on a 5 m × 5 m grid using a plant canopy analyzer (model LAI-2000, Li-Cor Biosciences, Lincoln, NE, USA).

Measurements of sapwood width (S_W) were obtained by the destructive sampling (i.e., felling at a height of 1.4 m) of 15 balsam fir trees with different diameters located outside the measurement plots. The conducting sapwood and inactive xylem were identified from the cut segment of the stem following the method of Coyea et al. [57] to obtain the allometric relationship between S_W or sap wood area (S_A) and DBH. These relationships are plotted in Figure 2 (with the associated coefficient of determination R^2) and were used to estimate sapwood area per unit of ground area (S_T).

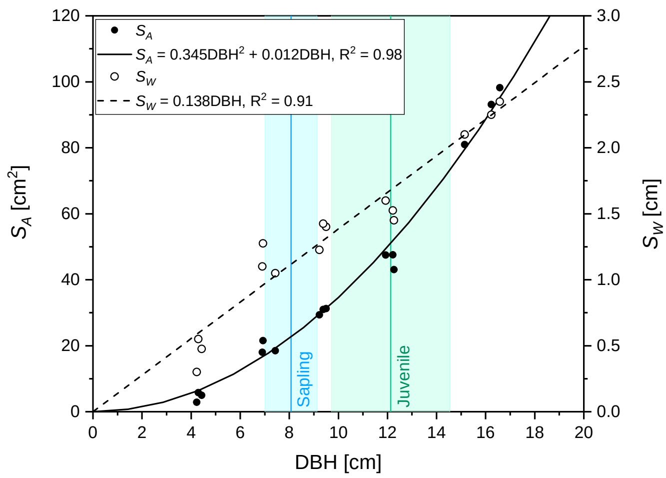

Figure 2. Allometric relationships between diameter at breast height (DBH) and sapwood area (S_A), as well as sapwood width (S_W) from 15 *Abies balsamea* trees located outside the measurement plots. Vertical green and blue lines are the average DBH of trees that were selected for sap flow measurements in Juvenile and Sapling site, respectively, whereas shaded areas represent standard deviations. Intercepts for linear and polynomial fits were forced to zero.

2.2. Eddy-Covariance and Micrometeorological Measurements

The Juvenile flux tower is 15-m high (≈1.5 times the mean canopy height) and is equipped with two identical sets consisting of a 3D sonic anemometer and an open path CO_2/H_2O analyzer (IRGASON, Campbell Scientific, Logan, UT, USA), both installed at a height of 14.63 m. The high-frequency sensors are facing opposite directions (303°, northwest; and 118°, southeast), so that time series from both devices can be combined depending on wind direction to minimize the effect of flow distortion by the tower structure. The Sapling flux tower is 10-m high and is equipped with a similar eddy-covariance system (IRGASON, Campbell Scientific, Logan, UT, USA) installed at a height of 8.5 m (≈1.5 times the mean canopy height). Each tower was also equipped with several meteorological instruments to measure net radiation (CNR4, Kipp & Zonen, Delft, The Netherlands), air temperature, and relative humidity (HC2S3 and HMP45C, Campbell Scientific, Logan, UT, USA). Total precipitation data was measured at a station located ≈ 4 km north of the study sites and operated by the Québec government [58]. Additional tipping bucket rain gauges (ECRN-100, Decagon, Pullman, WA, USA) were installed on each site during the sap flow measurement campaign and the readings were used to overwrite the data from the govermental weather station during that specific period of time.

Raw eddy-covariance data were processed using EddyPro® version 6.0 (Li-Cor Biosciences, Lincoln, NE, USA). Data processing routines followed the standard Fluxnet procedure, except for the coordinate rotation that used a sector-wise planar fit [59]. Notably, periods of rainfall were filtered out since rain droplets can obstruct the lenses of open-path gas analyzers. Gaps in the E time series caused by filtering procedures were filled using marginal distribution sampling as described in Reichstein et al. [60]. Remaining gaps were filled using monthly linear regression with zero-set intercept between E and net radiation.

2.3. Sap Flow Measurement

Sap flux densities were measured using commercially available Granier-type constant thermal dissipation probes (TDP-30, Dynamax, Houston, TX, USA) during two full growing seasons, from 5 July until 18 October in 2017 and 2018, when trees are actively transpiring. The starting date was a bit late due to several technical issues after the installation process at the beginning of April 2017. Each probe consists of a pair of 30-mm long needles (1.2 mm in diameter) installed one above the other. The upper one includes an electric heater and a thermocouple junction referenced to a junction in the lower needle [31]. The two needles were inserted radially into the sapwood and vertically separated by approximately 40 mm as suggested by the manufacturer [61]. The upper needle was heated with a constant voltage of 3 V using a voltage regulator (AVRD, Dynamax, Houston, TX, USA). The temperature difference (ΔT which is measured as electrical potential difference, in mV) between the two needles was measured every 60 s and recorded as 10-min averages on a CR10X (Campbell Scientific, Logan, UT, USA). ΔT is related to sap flux density (F_d): simply put, increasing sap flow decreases ΔT by cooling the heated needle [28,33].

Thermal dissipation probes were installed on balsam fir trees having stem diameter similar to that corresponding to the average DBH (Figure 2) at each site. Four adjacent trees were selected in each plot surrounding the Juvenile and Sapling flux tower. For three out of four trees, the needles were inserted on the north side of the tree to avoid heating from solar radiation. The fourth tree of each plot was equipped with probes on both the north and south sides to investigate potential circumferential variation. The probes were installed at a height of 1.4 m and 0.7 m above the ground at the Juvenile and Sapling plots, respectively. They were covered with a reflective insulation coating to prevent exposure to rain and direct sunlight [62,63], and to minimize the influence from ambient thermal gradient [28]. Adequate insultation is crucial to minimize uncertainties related to these three sources. The tree stems were covered from ≈ 15 cm above the upper probe down to the ground as suggested by Lu et al. [28].

Observed F_d is underestimated if part of the needles extends beyond the conducting sapwood depth, in which case the following correction has to be applied [40]:

$$\Delta T_{sw} = \frac{\Delta T - b\Delta T_{max}}{a} \tag{1}$$

where ΔT_{sw} is the temperature difference in the conducting sapwood only [mV], a and b are the fraction of needle in the conducting sapwood and the inactive xylem, respectively (i.e., $a + b = 1$), and ΔT_{max} is the maximum temperature difference between the two needles occurring when the flux is 0 for a given time period. This correction assumes that the thermal properties of inactive xylem are the same as those of the conducting sapwood when $F_d = 0$ [40]. Values of a and b for each sampled tree were estimated using the aforementioned relationship between DBH and sapwood width (Figure 2).

The F_d [$cm^3\ cm^{-2}\ h^{-1}$] was calculated using the Granier [33] power-type relationship with the flux index (K):

$$K = \frac{\Delta T_{max} - \Delta T_{sw}}{\Delta T_{sw}} \tag{2}$$

$$F_d = \alpha K^{\beta} \tag{3}$$

where α and β are calibration factors. Granier [33] found a strong correlation between K and F_d in two different conifer and one broad-leaf tree species, where α = 42.84 $cm^3\ cm^{-2}\ h^{-1}$ (0.0119 $cm^3\ cm^{-2}\ s^{-1}$ $\times$ 3600) and β = 1.231 [28,31,36]. Granier [33] stated that, based on the three species he studied, this empirical equation was not species-dependent [28]. However, other studies later found that for a given K, Granier's factors could underestimate F_d in several conifer tree species [36].

A combination of the environment-dependent method by Oishi et al. [29] and the daily maximum method by Granier [33] was used to estimate ΔT_{max} in Equation (2). The initial approach to define ΔT_{max} (daily maximum) was based on the assumption that $F_d = 0$ occurs every night, thus leading to the determination of ΔT_{max} on a daily basis [44]. Unlike the original approach, the environment-dependent method determines ΔT_{max} using actual environmental conditions by selecting the highest daily ΔT observed during conditions of low vapor pressure deficit (D). The advantage of the environment-dependent method is its ability to take into account seasonal shifts in ΔT_{max} and nocturnal water flux. However, this method requires high-humidity conditions (i.e., $D < 0.05$ kPa), which were not met on certain days. For these specific days, the daily maximum method was used as recommended by Rabbel et al. [44] for humid environments.

Ultimately, stand transpiration [$mm\ h^{-1}$] was calculated as:

$$E_T = \overline{F_d} S_T \tag{4}$$

where $\overline{F_d}$ is the mean sap flux density of sampled trees [converted in $L\ m^{-2}\ h^{-1}$, which is equivalent to $mm\ h^{-1}$] and S_T is the sapwood area per unit of ground area [$m^2\ m^{-2}$] [23,64]. The estimation of S_T can be obtained by applying the allometric relationship between DBH and S_A (Figure 2) to all trees within the plots [64].

2.4. Species-Specific Calibration of the Thermal Dissipation Approach for Sap Flow Measurements

In order to obtain the most accurate measurement of E_T, sap flow calibration was conducted in an environmentally-controlled laboratory by comparing gravimetric F_d with measurements of K using constant thermal dissipation probes [36]. Stem segments used for the calibration experiments were harvested from three different balsam fir trees of similar size (diameter $\approx$ 15 cm) located within the study site. The tree trunks were cut in length of 25 cm, wrapped in a wet cloth, and stored separately in black plastic bags to prevent dehydration during transportation and storage. A razor blade was used to trim both cut surfaces and to remove the top 2 cm of bark to ensure the water used for calibration only passed through the xylem [31]. Flow was induced from the top to the bottom of the reversed stem segment at a constant pressure-head using a Mariotte-based verification system, as described in Steppe et al. [31].

Before the start of the calibration procedure, each stem segment was covered by a plastic sheet to prevent dehydration and was maintained flow-less for 10 h to establish zero-flow conditions. K was measured by three constant thermal dissipation probes which were installed at the same height on three different sides of the stem segment (0°, 90°, and 180°). Flow was induced in the stem segment during a 2-h period to saturate the sapwood and stabilize probe readings before the start of the measurements. Calibration was then performed at constant pressure heads of 2.5, 5, 10, 15, and 25 cm for 45 min each time. Water dripping out at the bottom of the cut stem segment was weighted using an electronic balance (PM2500, Mettler Toledo, Toledo, OH, USA) and logged at a 1-min frequency to determine sap flow. The calibration curve was obtained by fitting a power function between K and gravimetric F_d.

2.5. Monitoring of Canopy Wetness

Wet and dry canopy conditions were determined using leaf wetness sensors (PHYTOS 31, METER Group, Inc., Pullman, WA, USA) from 5 July until 18 October in 2018. Leaf wetness sensors (LWS) monitor fluctuations in the dielectric constant of the sensor's upper surface to retrieve wetness [65]. A total of three LWSs were installed in plot J1 at three heights above the ground surface (2, 4, and 6 m) on branches ∼ 15 cm from the tree trunk. While the number of LWS used in this study was rather limited and their shape was not optimal to represent needles, they provided, based on our results (including visual assessment), a reasonable approximation of the general state of the canopy wetness. The LWSs were mounted at a 45° angle to simulate the typical position of the foliage and to prevent the accumulation of drops as recommended by the manufacturer [65]. The final output data is in raw counts (1 raw count = 1/0.733 mV measured using a datalogger with 3000 mV excitation), which ranged from 435 raw counts (dry) up to 1100 raw counts (saturated), and was stored on an EM50 Data Logger (METER Group, Inc., Pullman, WA, USA) at one minute intervals. Values $<$ 445 raw counts were considered as indicative of dry conditions and values $>$ 445 raw counts, of wet conditions.

Around a rainfall event, the canopy will undergo a "wetting–drying event" (t_{wd}), which consists of a wetting phase (t_w) and a drying phase (t_d). Data analysis included LWSs readings starting 30 min before the wetting phase (t_{w-1}) up to 30 min after the drying phase has ended (t_{d+1}). Based on the state of LWSs, the canopy wetness conditions were divided into four levels of wetness (W_L) as described in Figure 3. If all LWSs report dry conditions, the canopy is considered dry; if one of the LWSs report wet conditions, then the canopy is slightly wet; if two of the LWSs report wet conditions, then the canopy is fairly wet; and if all LWSs report wet conditions, then the canopy is considered wet.

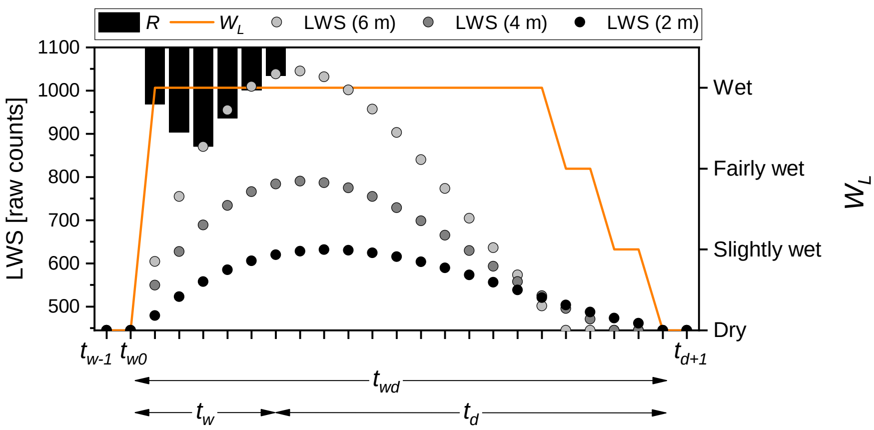

Figure 3. Conceptual translation of half-hourly LWS data to a canopy wetness level (W_L) during a wetting–drying event (t_{wd}). Wetting phase (t_w) is when the rain (R) $>$ 0 mm and drying phase (t_d) is when the rain has ceased but the canopy is not fully dry. t_{w-1} is 30 min before a wetting phase, t_{w0} is the starting point of a wetting phase, and t_{d+1} is 30 min after the end of a drying phase. The circles illustrate the evolution of canopy wetness at different heights above ground.

3. Results

3.1. Determination of E_T

3.1.1. Calibration of Sap Flow Measurements for Balsam Fir

The calibration process yielded 45 data points from each of the three stem segments (three sap flow sensors with a mean K value at each of the five constant pressure heads). Figure 4 shows the relationship between gravimetric sap flux density (F_d) and sap flux index (K). A power-type function, as with the original equation by Granier [33], was used to obtain the calibration curve where α = 54.997 cm^3 cm^{-2} h^{-1} and β = 1.204 (R^2 = 0.89). The coefficient of determination was slightly below that obtained by Granier [33] or other more recent sap flow calibration studies on coniferous-softwood type trees (e.g., [36,63]) where $R^2 \geq 0.95$, but was still deemed satisfactory. Note that this is the first time that calibration coefficients for the thermal dissipation method are being reported for balsam fir trees.

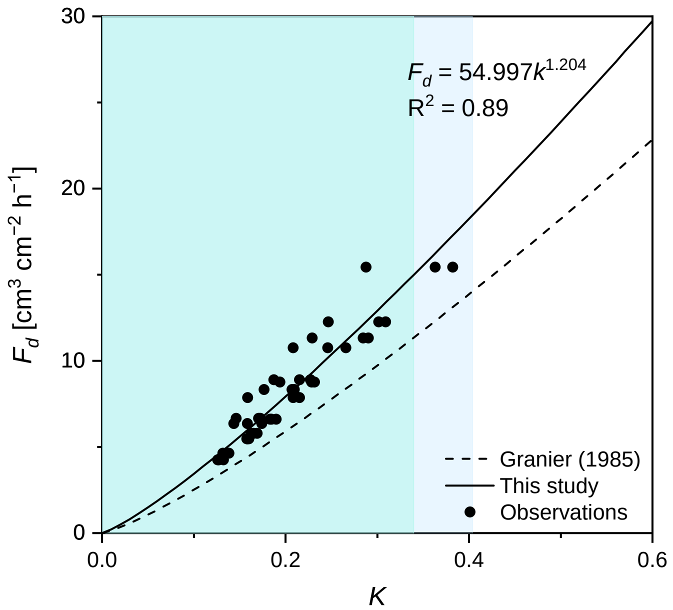

Figure 4. Sap flux density (F_d) vs sap flux index (K) of balsam fir stem segments (n = 3; each having 3 sap flow sensors × 5 pressure heads) obtained for this study, compared to the commonly used Granier's [33] calibration curve. The green and blue shaded area is the range of K values observed in Juvenile and Sapling sites, respectively.

3.1.2. Circumferential and Tree-to-Tree Variations

Other uncertainties related to the scaling process are from F_d variations across the azimuthal direction and between measured trees. Significant differences (p-value < 0.01) in F_d measured on the north and south sides of the trees were found in all plots during measurement period of 2017 and 2018. Nevertheless, none of the sampled trees (one in each plot) showed higher or lower F_d towards a specific azimuthal direction during the measurement periods (Figure 5a). Moreover, there were no meteorological parameters, nor soil water content fluctuations, from 2017 to 2018, which could explain the increase in circumferential variation. Overall, the coefficients of variation (CV) of F_d measured on north and south sides of the tree ranged from 32% to 47%.

Mean plot F_d values in this study were computed from four measurement trees. The tree-to-tree F_d variations within each site were significantly different (p-value < 0.01) both in Juvenile and Sapling throughout two measurement periods. The deviation of each tree F_d from the site mean was variable, as represented by 1.5× the interquartile range (IQR) in Figure 5b. The observed F_d values of in Juvenile plots had slightly higher CVs, 52% to 57%, compared to those in Sapling plots, 44%.

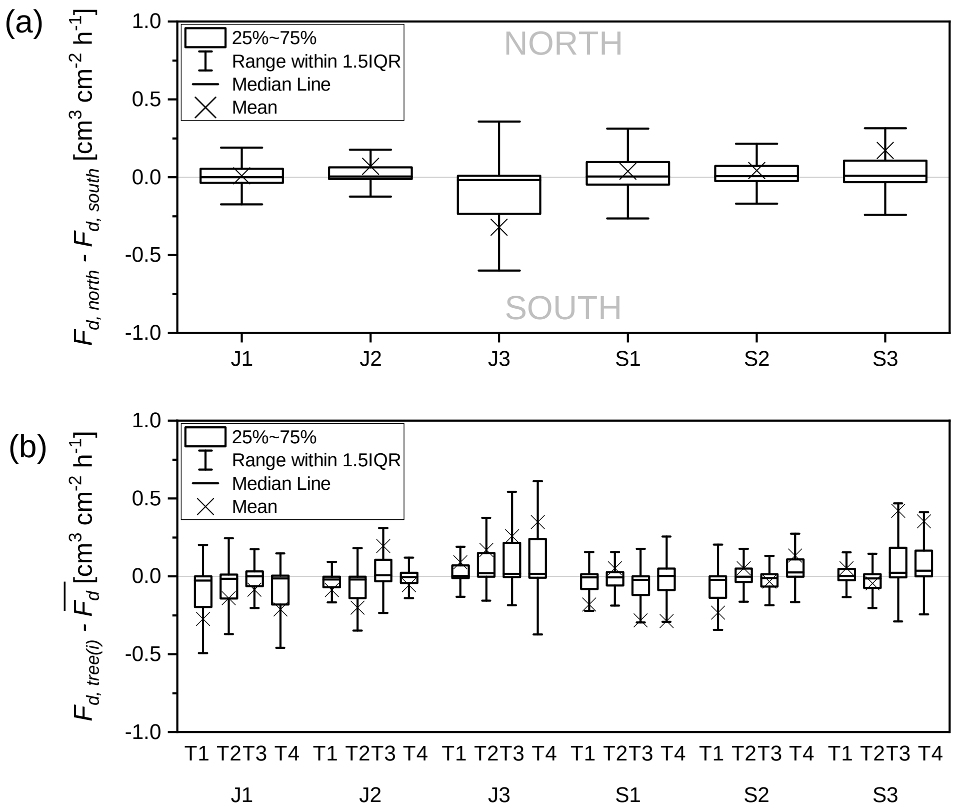

Figure 5. (**a**) Distribution of sap flux density (F_d) differences between sensors installed on south and north sides of the tree; and (**b**) tree-to-tree variations described by the deviation of each tree F_d from the site mean F_d. The variability is described by the interquartile range (IQR). Letters on the *x*-axis refer to tree (T), Juvenile (J) and Sapling (S), and followed by the tree or plot number.

3.2. Characteristics of Wetting–Drying Events

As many as 30 wetting–drying events were recorded from 5 June 2018 until 18 October 2018 at Juvenile site. A total of 482 mm of rain fell during this period. The wetting–drying events were characterized by lower net radiation (R_n; 59 $\pm$ 121 W m^{-2}) and vapor pressure deficit (D; 0.09 $\pm$ 0.14 kPa) than during dry canopy conditions, 91 $\pm$ 186 W m^{-2} and 0.41 $\pm$ 0.34 kPa, respectively.

The length of each wetting–drying event (t_{wd}) was quite variable, ranging from 4 h up to 116.5 h, and was weakly correlated with the total amount of rain (R) during the event (R^2 = 0.46). However, the relationship between the length of wetting phase (t_w) and R was quite strong (R^2 = 0.83), as one would expect. In most cases, the wetting phase lasted less than 10 h, which was long enough to wet LSW at all three heights (Figure 6a,c). For 25 out of 30 events, rainfall led to a completely wet canopy, whereas in the remaining five cases, the canopy only reached fairly and slightly wet states (see Table A1 for details).

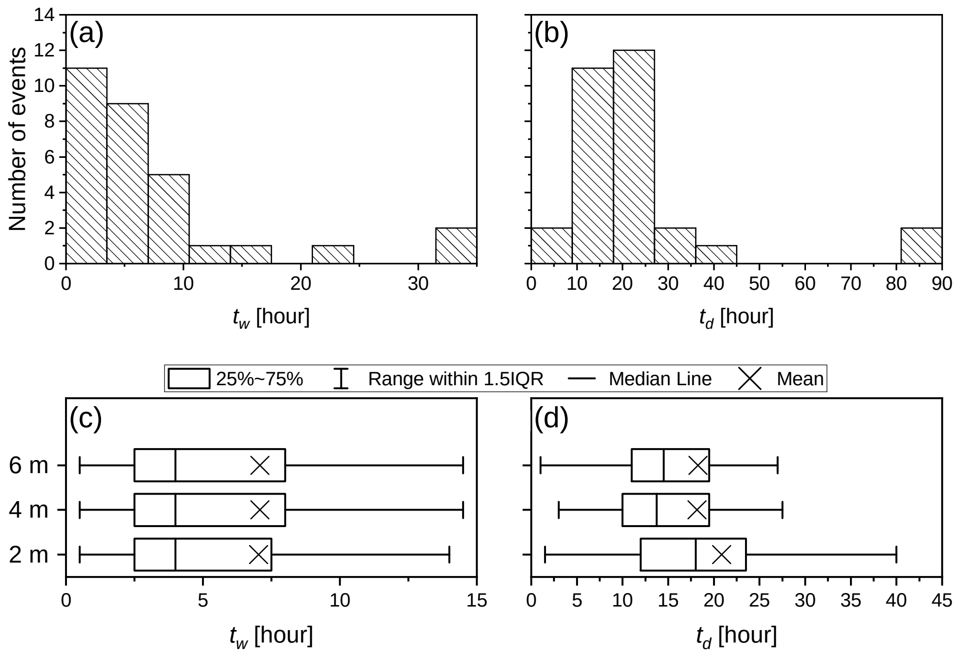

Figure 6. Characteristics of (**a**) wetting (t_w) and (**b**) drying (t_d) phases duration described by histograms of t_w and t_d; as well as the vertical distribution of (**c**) t_w and (**d**) t_d between LWS installed at three different heights: 2, 4, and 6 m. The variability is described by the interquartile range (IQR).

On the other hand, the length of the drying phase (t_d) and the amount of time required to completely dry all three LWSs ranged from 3 h up to 84.5 h (Figure 6b,d). The LWS at 2 m required longer time to dry compared to LWSs at 4 m and 6 m. We used multiple linear regressions to estimate the length of drying phases (t_d [hour]) with average net radiation (R_n [W m^{-2}]), vapor pressure density (D [kPa]), and wind speed (u [m s^{-1}]) as predictors. The model took the following form:

$$t_d = 0.056R_n - 21.5D + 14.1u \tag{5}$$

and had an R^2 value of 0.51 (p-value $= 4 \times 10^{-5}$). To accurately estimate the drying phase duration requires another element, which is the amount of rain stored in the canopy. Not all of the rain is intercepted by the forest canopy as a fraction passes through canopy gaps and reaches the forest floor.

3.3. Dynamics of E_T and E_T/E during Wetting–Drying Events

Daily courses of E and E_T during two typical wetting–drying events show that both variables decrease when the forest canopy is progressively wetted by precipitation (Figure 7). Surprisingly, a rainfall accumulation of only 0.4 mm received on 15:30 of 17 August 2018 was sufficient to put the canopy in a wet state and reduce E and E_T by 6% and 7%, respectively (Figure 7a). Meanwhile, 30.8 mm of rainfall received over $\sim$ 14 h during daytime on 22 August 2018 reduced daily cumulative E and E_T by 86% and 116%, respectively, compared to the day after that rain event. Once the canopy started to dry, E gradually increased followed by E_T.

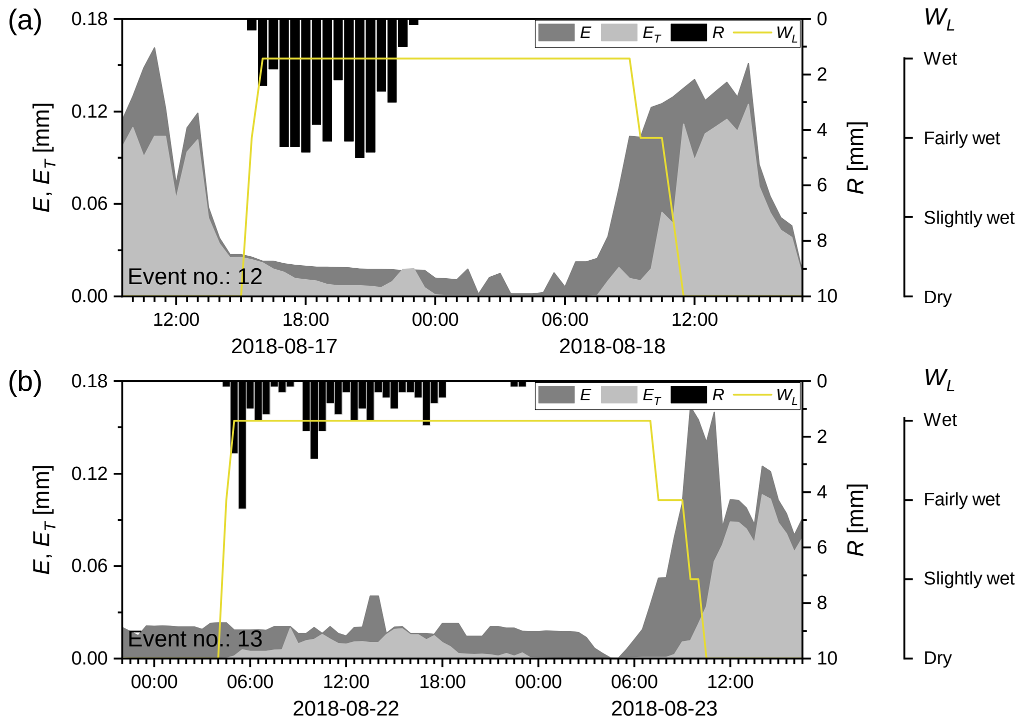

Figure 7. Effect of rain events (R) from (**a**) 15:30 until 23:00 of 17 August 2018 and from (**b**) 04:30 until 18:00 of 22 August 2018 on half-hourly canopy wetness level (W_L), evapotranspiration (E), and transpiration (E_T).

Figure 8a shows decreases in E_T under various canopy wetness stages compared to that during dry canopy conditions. For instance, the average E_T was 70% lower under wet canopy conditions during the wetting phase (t_w) than during the half-hour before (t_{w-1}). Interestingly, under wet canopy conditions, E_T values were slightly higher during the wetting phase (0.007 $\pm$ 0.009 mm) than those during the drying phase (0.004 $\pm$ 0.008 mm). During the wetting phase, the rain was able to wet all three LWSs resulting in a canopy wetness level categorized as "wet" although the canopy was not fully saturated. On the other hand, at the beginning of a drying phase, the canopy was mostly wet due to rain accumulation during the wetting phase. Once the canopy wetness reached fairly and slightly wet conditions, the mean E_T increased to 0.010 $\pm$ 0.016 mm and 0.022 $\pm$ 0.028 mm, respectively. Thirty minutes after the canopy became dry (t_{d+1}), the average E_T was 70% higher than during the t_{w-1} period.

Under wet canopy conditions, E_T/E decreased in a similar fashion as E_T (Figure 8b). E_T/E declined from 0.44 $\pm$ 0.29 half an hour before rainfall to 0.31 $\pm$ 0.32 under wet canopy conditions in the wetting phase. Once the rain ceased and the canopy was still in fully wet conditions, E_T/E further dropped to 0.16 $\pm$ 0.22. Even if the canopy starts to dry, transitioning from "wet" to "fairly wet", E_T/E reached its lowest value (0.14 $\pm$ 0.15). The low E_T/E values observed under fairly wet conditions were due to E increasing at a higher rate than E_T. Once the canopy was under slightly wet conditions, E_T/E rose to 0.35 $\pm$ 0.31. While the changes in E_T/E ratio during wetting–drying events were similar to those of E_T, the difference of E_T/E between the t_{w-1} and t_{d+1} periods was only 13%.

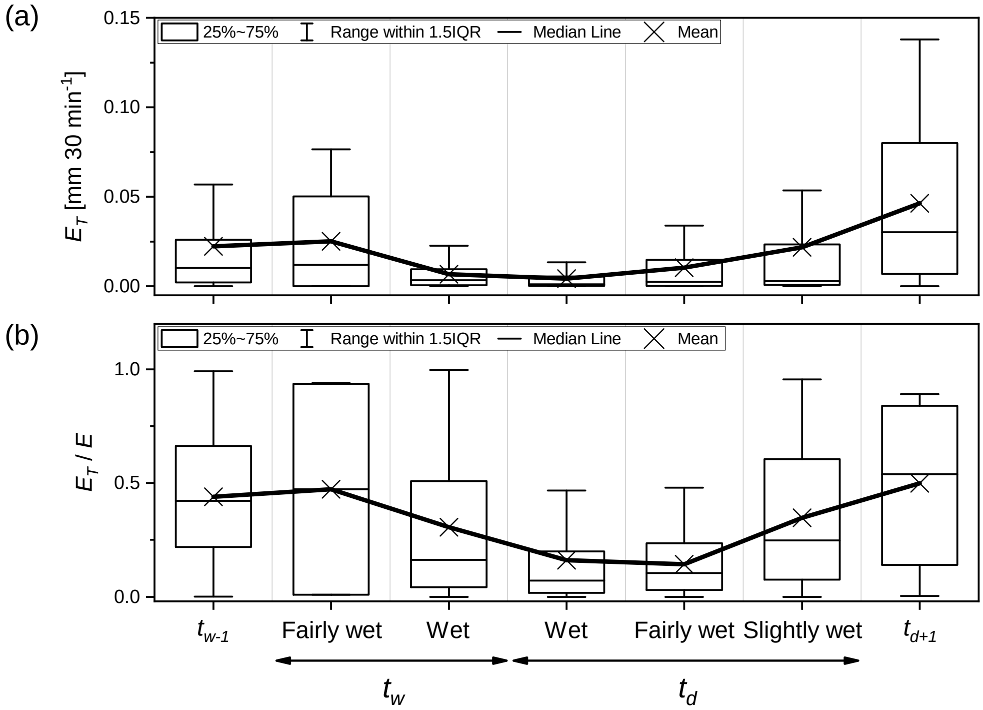

Figure 8. Variations of (**a**) E_T and (**b**) E_T/E before wetting phase (t_{w-1}), during wetting (t_w) and drying (t_d) phases as well as after the canopy became completely dry (t_{d+1}). E_T and E_T/E variability is described by the interquartile range (IQR). The solid bold lines are connecting the means of each phase.

3.4. E_T/E at the Seasonal Scale

Figure 9 presents a summary of seasonal values for evapotranspiration (E), transpiration (E_T) and transpiration to evapotranspiration ratio (E_T/E) measured at Juvenile and Sapling sites from 5 July to 15 October in 2017 and 2018. In 2017, Juvenile and Sapling sites received 509 mm and 462 mm of rainfall, respectively, whereas in 2018 the total rainfall was 482 mm at the Juvenile site and 452 mm at the Sapling site. Despite having received less rainfall in 2018, there was a significant decrease (∼21%) in E at the Juvenile site (from 246 mm in 2017 to 200 mm in 2018). In contrast, E at the Sapling site slightly increased from 211 mm in 2017 to 220 mm in 2018. The evaporative index, i.e., the ratio of evapotranspiration to precipitation (E/P) or rain (E/R), decreased in Juvenile site and increased in Sapling site between 2017 and 2018. The summary from two years of measurement period shows a quite similar E/R ratio between Juvenile (0.45) and Sapling (0.48) site.

Transpiration from young balsam fir stands, the dominant vegetation at the study site, was not the major contributor to evapotranspiration. Only 0.42 ± 0.04 and 0.28 ± 0.01 of E was attributable to aboveground E_T in Juvenile and Sapling sites, respectively, in 2017. In 2018 the proportion of E_T to E increased by 25% in Juvenile and 40% in Sapling. Overall, the increases in E_T/E between years were almost similar to those of E/R with a gain of 18% at the Juvenile site and 48% at the Sapling site.

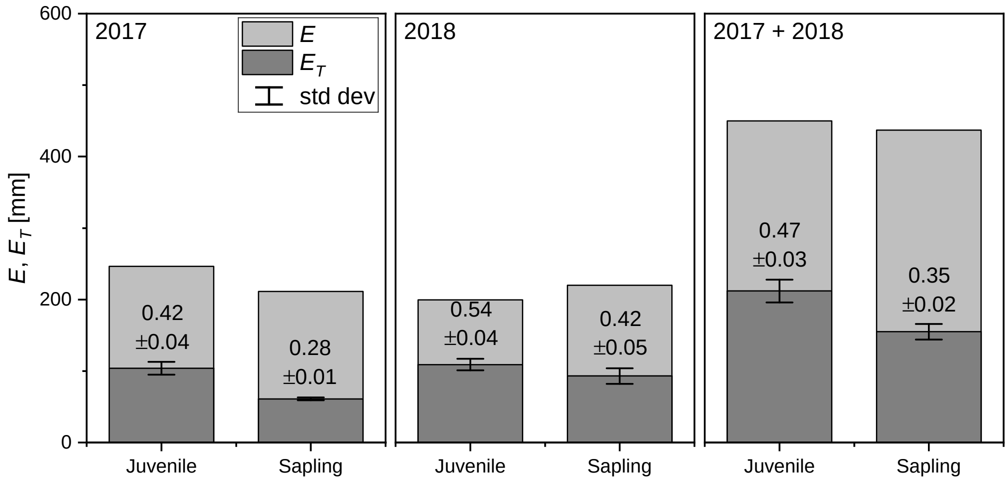

Figure 9. Summary of evapotranspiration (E) and transpiration (E_T) from 5 July to 18 October in 2017 and 2018. The numbers above E and E_T bars are mean E_T/E values ± standard deviation.

4. Discussion

4.1. Sources of Uncertainty in E_T

In this study, we measured tree transpiration using the thermal dissipation method and upscaled sap flux density (F_d) from sampled trees to stand transpiration (E_T). During the measurement and calculation process, we applied a series of corrections, including species-specific calibration to improve the accuracy and minimize the uncertainty in E_T. Our calibration using 25-cm long balsam fir stem segments resulted in a significantly higher F_d value for a given K than that provided by Granier's empirical equation (t-test, $\alpha = 0.05$, p-value < 0.001).

Previous studies have also shown that Granier's [33] calibration coefficients may underestimate F_d for several evergreen conifer species such as *Pinus elliottii*, *Pinus palustris*, *Picea abies*, and *Pinus sylvestris* [36,39,63]. Compared with these studies, our calibration curve resulted in F_d values that were 5%–23% higher than those reported by Bosch et al. [39] and Peters et al. [36] for *Pinus elliottii*, *Pinus palustris*, and *Picea abies* at K values ranging between 0 and 0.4 (similar to that observed during the calibration process). Overall, our calibration coefficients increased F_d values estimated using Granier's coefficients by 34 ± 8%. This finding is similar to results by Lundblad et al. [63], who reported a 40% increase in E_T when using species-specific calibration factors for *Picea abies* and *Pinus sylvestris* trees.

Another uncertainty from sap flow measurements is the location of sensors installed on the tree trunk. This study was conducted in the Northern Hemisphere where the southern part of the tree canopy receives more sunlight, and hence is expected to transpire more than the shaded counterpart [66]. However, we found no systematic variation in F_d between sensors installed on north versus south side of the tree. While this might be related to height differences among individual neighbor trees, thus creating a shading effect on measured trees, many studies have also found non-systematic circumferential variations in F_d (e.g., [67–69]), yet the reason behind these variations has not been adequately identified [68,70]. These results suggest that the water lost through transpiration on one side of the tree crown might not come from the xylem on the same side. Indeed, for most types of conifers, the hydraulic transport network is composed of tracheids with bordered pits, which allow water to move easily in the tangential direction [71]. Nevertheless, Saveyn et al. [43] emphasized the importance of installing sap flow probes at multiple points around the stem circumference to reduce errors and obtain a more precise scaling of tree E_T.

Variations in F_d were also found in a measurement plot from one tree to the other. We could not pinpoint any factor responsible for the tree-to-tree F_d variation. However, several previous studies (e.g., [30,72,73]) showed that the variation in F_d between trees was closely related to tree size which was affected by competition among trees for water and sunlight in the stand. The uncertainty caused by spatial variability between plots can be reduced by sampling more trees or plots [74]. The standard errors of the mean are then computed to obtain a value of uncertainty in the cumulative E_T using summation in quadrature, commonly known as square root of the sum of squares.

4.2. Dynamics of E_T and E during Wetting–Drying Events

In this study, the wetting–drying events were monitored using leaf wetness sensors (LWS) that had a different shape and much larger surface area than balsam fir needles. Leaf wetness sensors have been used to analyze the effect of canopy wetness on transpiration (e.g., [22,75,76]) due to its ease of use. Although the sensors are clearly not suitable to quantify the exact amount of water stored in the canopy during a wetting–drying event, they are used here to provide a qualitative description of the canopy wetness. We also must remind readers that due to logistical constraints, only one tree was monitored using three LWS installed at three different heights. Despite the aforementioned limitations, the LWS sensors were able to estimate the timing of wetting and drying phase, in line with the decrease and increase of E_T and E related to the canopy wetness during all wetting–drying events. Three completely independent measurement methods (sap flow, eddy-covariance and LWS) were able to provide a rather clear picture of the phenomena taking place around a rainfall event. Nevertheless, to precisely quantify canopy wetness requires specific methods to measure the amount of rain intercepted by the canopy and its evaporation as explained in a study by Rutter et al. [77]. We did not include the method mentioned earlier in this study because of its complexity to estimate the canopy wetness in time series.

The decreases and increases in E_T around wetting–drying events were closely related to net radiation (R_n) and vapor pressure deficit (D). The lower E_T rate in the pre-wetting phase compared to that in the post-drying phase after the drying phase is due to the presence of clouds, resulting in low R_n, and low D. The E_T rate is regulated by stomatal conductance, and in the case of abundant soil water, it depends on R_n and D. Figures 10a,b show different responses of E_T under dry canopy conditions to D during daytime ($R_n > 10$ W m^{-2}) and nighttime ($R_n < 10$ W m^{-2}). The relationship between E_T and D was higher during daytime ($R^2 = 0.58$) compared to nighttime ($R^2 = 0.17$), because on several occasions, D was quite high over night while the sap flow had already reached zero.

Contrary with the study by Cienciala et al. [21] who found a strong correlation between E_T and D under wet canopy conditions, the weak relationships between both parameters in this study suggest that the presence of rain drops on the tree needles do play a role in 'regulating' tree E_T rate. A rainfall accumulation of 0.2 mm on dry canopies during the first half-hour of the wetting phase ($R(t_{w0})$) was able to reduce E_T on four out of 10 occasions. The reduction rate of E_T caused by the rain was not clear until $R(t_{w0})$ was greater than 1 mm (Figure 11). This could provide a first estimation of the amount of rain needed to saturate the canopy. However, forest canopies only intercept a fraction of the total rain, depending on the closeness of the canopies. A specific method is required to estimate the amount of rain that is intercepted by the canopy during rainfall events.

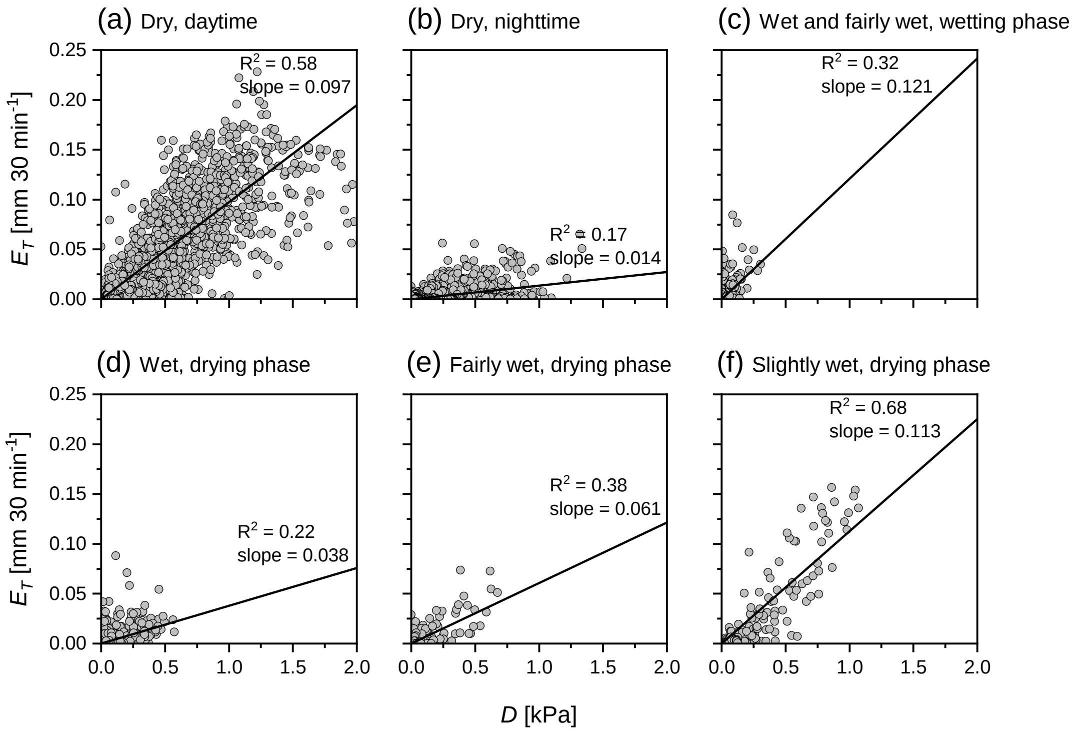

Figure 10. Relationships of half-hourly data between vapor pressure deficit (D) and transpiration (E_T) at the Juvenile site under different canopy conditions: (**a**) dry during daytime ($R_n > 10$ W m^{-2}), (**b**) dry during nighttime ($R_n < 10$ W m^{-2}), (**c**) wet and fairly wet during wetting phases, (**d**) wet during drying phase, (**e**) fairly wet canopy during drying phase, and (**f**) slightly wet during drying phase.

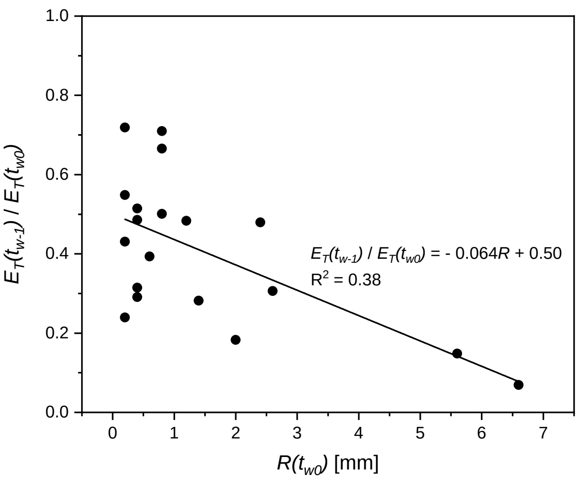

Figure 11. Reduction of E_T in response to canopy humidification due to rain in the first half-hour of wetting phases ($R(t_{w0})$), described with ratio of E_T during pre-wetting phase ($E_T(t_{w-1})$) and the first half-hour of wetting phase ($E_T(t_{w0})$). Only $E_{T(tw-1)}/E_{T(tw0)} < 1$ were used for the analysis.

The strong correlation between E and E_T under dry canopy conditions (R^2 = 0.70) and weak correlation under wet canopy conditions (R^2 = 0.23) is in line with the study of Granier et al. [23] (R^2 = 0.85 under dry canopy conditions and R^2 = 0.46 under wet canopy conditions). We did not find any time lag between both parameters under any canopy conditions, nor on the relationship between sap flow measurements and D (for details see Table A2). In a previous study by Saugier et al. [78], a 1.5 h lag was found between E_T measured using branch bag at the canopy level and sap flow measurements. This time lag was caused by changes in wood water storage and by sap flow measurement position (1.3 m). The absence of lag (or presence of a lag < 30 min) between sap flow measurements and E from eddy-covariance measurements implies that the change of water storage happens quickly in young balsam fir trees.

E_T/E itself varies during the wetting–drying events, showing that the rain also reduces E but not in the same proportion as E_T. The lower E_T/E during the drying phase, especially in wet and partially wet conditions, indicates that the most dominant E component during these periods was E_C (with the assumption of E_G occupying a relatively constant proportion of E). E_C was noticeable during the wetting phase and became more dominant after the rainfall had ceased.

4.3. Eddy-Covariance during Rainfall

Unlike the sap flow method, eddy-covariance measurements used in this study rely on open-path sensors that cannot record reliable measurements during rainfall [23]. For this reason, this study relies on the gap filling method (marginal distribution sampling) to obtain E during the wetting–drying events. By design, marginal distribution sampling fills the data gaps with E values of periods with similar meteorological conditions, based on net radiation (R_n), air temperature (T_a), and vapor pressure deficit (D). We evaluated marginal distribution sampling performance by creating 1000 artificial gaps on the half-hourly time series during dry canopy conditions apart from the the existing gaps that have similar meteorological conditions during wetting–drying events. These artificial gaps covered ~20% of the available data. Marginal distribution sampling only slightly underestimated the actual observation values and performed well (Figure 12). These results greatly improved our confidence in the gap-filling technique used to estimate E during wetting–drying events.

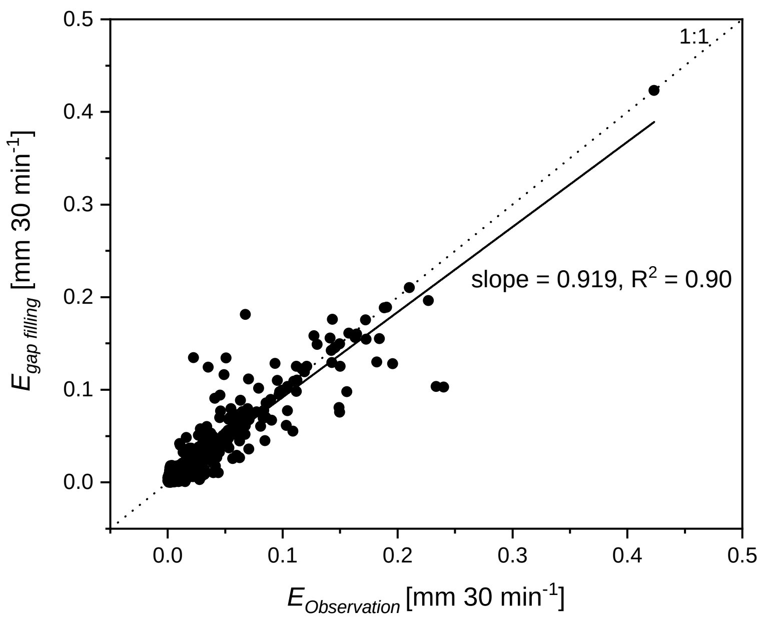

Figure 12. Comparison between marginal distribution sampling to fill artificial gaps of E under similar meteorological conditions during wetting–drying events, and the actual observation from eddy-covariance system ($n = 1000$).

4.4. E_T/E at the Seasonal Scale

The cumulative rainfall at the Juvenile site during the measurement period of 2018 was 5% less than in 2017. The decrease in rainfall was not followed by an increase of net radiation (R_n) or vapor pressure deficit (D): on the contrary, the averages of R_n and D decreased by 9% and 12%, respectively. This resulted in the reduction of E but increased E_T by 5% compared to 2017. At the Sapling site, R_n and D increased from 2017 to 2018 by 2% and 31%, respectively, leading to an increase of E_T by 42%. These results suggest that the magnitude of E_T is not only regulated by meteorological conditions, but also influenced by the growth of both young stands. A study by Tyree [79] demonstrated that stand growth is an important influence on the E_T rate.

The age difference between stands at the Juvenile and Sapling sites are especially outlined by the difference in DBH and LAI. The Sapling site younger stands had a E_T/E ratio 29% lower compared to the Juvenile site for both years. The difference in E_T/E between sites was likely related to LAI, which was $\approx$ 22% lower at the Sapling site. This finding is similar to that of a study by Breda et al. [80], where E_T is not correlated with DBH, but more related to LAI. Furthermore, Granier et al. [81] found that a reduction in LAI was associated with a decrease in E_T in open stands as a result of the reduction of the transpiring canopy surface, and that it was not associated with a decrease of total E. Other studies have also determined that changes in LAI could alter E partitioning in E_G and E_T by regulating the ratio between area covered by the canopy and stands opening [82–85].

Globally, values of E_T/E in this study appear lower than the summary of several studies in boreal forests by Schlesinger and Jasechko [17], in which $E_T/E = 65\% \pm 18\%$. However, in several studies that directly measured E_T/E in boreal and temperate forests we could find (Table 2), E_T represented less than 50% of E, suggesting that E_C and/or E_G were quite significant. Interestingly, there is no clear relationship between LAI and E_T/E. Despite only having a LAI of 2.3, the E_T of a trembling aspen stand in Prince Albert National Park, Canada, represented 95% of E [49]. On the other hand, with LAI value ranging from 9.4 to 14.2, E_T of a Eastern white pine stand in Coweeta Basin, US, only represented 55% of E [74].

Compared to the other existing E_T/E studies in boreal forest, Montmorency Forest has the highest precipitation (P), even higher than several studies in temperate regions we found (Table 2). Despite high precipitation, only $45\% - 48\%$ returns back to the atmosphere. Isabelle et al. [20] in a study at the same sites found that E appeared to be capped even in the presence of high precipitation. The excess of P generates runoff or recharge of ground water, indicating that the availability of soil water is probably not a limiting factor for E_T. In the absence of limitation from soil water availability, LAI appears to be a better proxy to estimate E_T/E at the seasonal scale.

Table 2. Comparison of LAI, E_T/E, annual precipitation (P) and evaporative index (E/P) between this study and several previous studies of E partitioning in boreal and temperate forests. Sites are ordered by annual precipitation rate, from the site receiving the most precipitation to the site receiving the less precipitation

Site	Climatic Zone	Vegetation	Study year(s)	LAI [$m^2\ m^{-2}$]	E_T/E	Annual P [$mm\ y^{-1}$]	E/P	Reference
Coweeta Basin, US	Temperate	Eastern white pine	2004–2005	9.4–14.2	0.55 *	2241	0.65 *	[74]
Kahoku, Japan	Temperate	Japanese cedar, Japanese cypress	2007–2008	3.6–5.2	0.43 *	2138	0.39 *	[86]
This study (Juvenile)	Boreal	Balsam fir	2017–2018	3.6	0.47 **	1583	0.45 *	
This study (Sapling)	Boreal	Balsam fir	2017–2018	2.9	0.35 **	1583	0.48 *	
Walker Branch Watershed, US	Temperate	Mixed forest	1998–1999	6	0.43 *	1333	0.50 *	[24]
Duke Forest, US	Temperate	Mixed forest	2002–2005	7	0.56 *	1146	0.56 *	[29]
Lägeren, Switzerland	Temperate	Mixed forest	2014–2015	1.7–5.5	0.74 *	1037	0.87 *	[87]
Vielsalm, Belgium	Temperate	Mixed forest	2010–2011	4.1–5	0.68 **	1000	0.35 *	[48]
Krycklan, Sweden	Boreal	Mixed forest	2016	4.4–5.2	0.44 **	619	0.86 **	[88]
Norunda, Sweden	Boreal	Norway spruce	1995	4–5	0.65 **	527	1.29 **	[5]
Prince Albert Nat. Park, Canada	Boreal	Trembling aspen	1994	2.3	0.95 **	463	0.89 **	[49]
Scotty Creek, Canada	Boreal	Black spruce	2013	0.9–0.3	0.02 **	390	0.76 *	[19]

* during a full year; ** during a particular period in a growing season.

5. Conclusions

This study aims to investigate the dynamics of transpiration (E_T) to evapotranspiration (E) ratio (E_T/E) under wet and dry canopy conditions at two measurement sites in Montmorency Forest, a unique boreal forest with abundant precipitation and high E. Studying the variations of E_T/E across different canopy wetness conditions is essential, especially for model development to simulate E partitioning. Half-hourly E, E_T, and leaf wetness status were measured using eddy-covariance, sapflow (thermal dissipation method), and LWS. The thermal dissipation sensors were calibrated using trunk samples from balsam fir trees and led to new calibration coefficients ($\alpha = 54.997$ cm^3 cm^{-2} h^{-1} and $\beta = 1.204$).

The amount of time needed to completely dry the canopy was 22 ± 18 h, and was influenced by net radiation, vapor pressure deficit, wind speed, and the amount of rain intercepted by the canopy. Apart from the low vapor pressure deficit and net radiation during the wetting–drying phases, the presence of water on balsam fir needles decreased E_T. During the wetting–drying events, E_T/E ranged from $14 \pm 15\%$ to $47 \pm 54\%$, depending on the wetness level of the canopy.

At the seasonal scale, the variation of E_T/E between our two measurement sites was likely related to differences in leaf area index (LAI). Compared to the several studies of E and E_T partitioning in boreal and temperate forests, we found that our study sites were among several sites in which E_T was not the major component of E. Based on those studies, LAI appears to be a better proxy to estimate E_T/E, although it is not always the case.

This study focused on the dynamics of E_T/E at different levels of canopy wetness. However, a proper method is required to estimate the amount of water stored on the canopy during wetting–drying events and the drying rate at half-hourly time steps. Future studies should address the time series of E partitioning, especially the transition of E_T and E_C from wet to dry and dry to wet canopy conditions.

Author Contributions: Conceptualization, B.H., S.P., and D.F.N.; Methodology, B.H., S.P., and D.F.N.; Software, B.H. and P.-E.I.; Validation, B.H. and P.-E.I.; Formal analysis, B.H. and P.-E.I.; Investigation, B.H. and P.-E.I.; Resources, S.P. and D.F.N; Data curation, B.H. and P.-E.I.; Writing–original draft preparation, B.H.; Writing–review and editing, S.P., P.-E.I., and D.F.N.; Visualization, B.H.; Supervision, S.P. and D.F.N.; Project administration, D.F.N.; Funding acquisition, D.F.N. All authors have read and agreed to the published version of the manuscript.

Funding: This research was funded by the Natural Sciences and Engineering Research Council of Canada (NSERC), Ouranos Consortium, Hydro-Québec, Environment and Climate Change Canada, and Ministère de l'Environnement et de la Lutte contre les Changements Climatiques (MELCC), through NSERC project RDCPJ-477125-14, and by the Fonds de recherche du Québec - Nature et Technologies (FRQNT).

Acknowledgments: The authors would like to thank Annie-Claude Parent, Laurie Mignault, Achut Parajuli, Simon Lachapelle, Adrien Pierre, Judith Fournier, Kelly Proteau, Benoit Brault, Alicia Talbot-Lanciault, Gonzalo Leonardini Quelca, and Benjamin Bouchard for their help during field work and maintaining the micrometeorological towers. We also want to thank Antoine Thiboult for the valuable advice on uncertainty analysis and Carole Coursolle for insightful comments on the manuscript.

Conflicts of Interest: The authors declare no conflict of interest. The funders had no role in the design of the study; in the collection, analyses, or interpretation of data; in the writing of the manuscript, or in the decision to publish the results.

Appendix A

Table A1. Characteristics of each wetting–drying event described by the total rain (*R*) during event, length of the event (t_{wd}), length of wetting phase (t_w), length of drying phase (t_d) and contribution of each canopy condition in Juvenile during the measurement period of 2018.

Event	R	t_{wd}	t_w/t_{wd}	t_d/t_{wd}	t_w			t_d		
					Slightly Wet	Fairly Wet	Wet	Wet	Fairly wet	Slightly Wet
	[mm]	[hour]	[%]	[%]	[%]	[%]	[%]	[%]	[%]	[%]
1	11	17	15	85	-	-	100	100	-	-
2	7.8	35.5	23	77	-	-	100	93	-	7
3	13.2	29	14	86	-	-	100	98	2	-
4	78.2	116.5	27	73	-	-	100	91	8	1
5	4	19.5	5	95	-	-	100	81	19	-
6	16.6	15	27	73	-	-	100	95	5	-
7	3.6	28.5	9	91	-	-	100	75	4	21
8	3.8	10.5	10	90	-	-	100	58	21	21
9	11.2	24.5	18	82	-	11	89	90	5	5
10	6	21	17	83	-	-	100	54	29	17
11	0.8	4	13	88	-	-	100	29	14	57
12	50	20	40	60	-	6	94	83	13	4
13	31.2	30	48	52	-	3	97	81	13	6
14	1	23.5	6	94	-	-	100	82	2	16
15	4	23	15	85	-	-	100	67	5	28
16	8.2	20.5	12	88	-	-	100	81	6	14
17	9.4	26.5	26	74	-	-	100	97	3	-
18	1.2	19.5	5	95	-	-	100	95	-	5
19	9	13.5	22	78	-	-	100	100	-	-
20	5	40	23	78	-	-	100	87	2	11
21	12	16	28	72	-	-	100	65	35	-
22	0.6	25	4	96	50	-	50	56	-	44
23	27.2	25	52	48	-	-	100	79	13	8
24	43.4	47	50	50	-	-	100	51	34	15
25	8.8	18.5	35	65	-	-	100	38	17	46
26	2.4	15	17	83	-	-	100	52	20	28
27	4.6	26	13	87	-	-	100	53	7	40
28	6.8	44.5	10	90	-	11	89	34	1	65
29	69.6	114.5	29	71	-	-	100	71	1	28
30	8.6	10.5	71	29	-	-	100	100	-	-

Table A2. Relationships of half-hourly E_T measured using sap flow with E and D measured from the flux tower, under various canopy conditions and increasing values of time lag.

	Time Lag [hour]	All	Dry	Wetting–Drying Events			
				Wetting Phase	Drying Phase		
					Wet	Fairly Wet	Slightly Wet
E [mm 30 min^{-1}] vs. E_T [mm 30 min^{-1}]							
R^2	0	0.67	0.82	0.32	0.31	0.46	0.64
	0.5	0.66	0.78	0.25	0.32	0.34	0.66
	1	0.67	0.77	0.22	0.29	0.24	0.63
	1.5	0.65	0.72	0.21	0.28	0.17	0.55
	2	0.61	0.65	0.20	0.22	0.15	0.48
Slope	0	0.59	0.70	0.22	0.11	0.19	0.51
	0.5	0.58	0.69	0.18	0.11	0.16	0.51
	1	0.59	0.68	0.16	0.10	0.13	0.50
	1.5	0.58	0.67	0.15	0.10	0.11	0.46
	2	0.57	0.65	0.14	0.09	0.08	0.43
D [kPa] vs. E_T [mm 30 min^{-1}]							
R^2	0	0.54	0.48	0.32	0.22	0.38	0.68
	0.5	0.51	0.45	0.28	0.22	0.26	0.57
	1	0.48	0.41	0.26	0.20	0.18	0.49
	1.5	0.44	0.37	0.25	0.18	0.13	0.44
	2	0.39	0.33	0.24	0.17	0.13	0.41
Slope	0	0.08	0.08	0.12	0.04	0.06	0.11
	0.5	0.08	0.08	0.11	0.04	0.05	0.11
	1	0.08	0.08	0.10	0.03	0.04	0.10
	1.5	0.07	0.07	0.09	0.03	0.03	0.09
	2	0.07	0.07	0.09	0.03	0.03	0.09

References

1. Dixon, R.K.; Solomon, A.M.; Brown, S.; Houghton, R.A.; Trexier, M.C.; Wisniewski, J. Carbon pools and flux of global forest ecosystems. *Science* **1994**, *263*, 185–190. [CrossRef] [PubMed]
2. Bonan, G.B. Forests and climate change: Forcings, feedbacks, and the climate benefits of forests. *Science* **2008**, *320*, 1444–1449. [CrossRef] [PubMed]
3. Baldocchi, D.; Kelliher, F.M.; Black, T.A.; Jarvis, P. Climate and vegetation controls on boreal zone energy exchange. *Glob. Change Biol.* **2000**, *6*, 69–83. [CrossRef]
4. Kropp, H.; Loranty, M.; Alexander, H.D.; Berner, L.T.; Natali, S.M.; Spawn, S.A. Environmental constraints on transpiration and stomatal conductance in a Siberian Arctic boreal forest. *J. Geophys. Res.* **2017**, *122*, 487–497. [CrossRef]
5. Grelle, A.; Lundberg, A.; Lindroth, A.; Morén, A.-S.; Cienciala, E. Evaporation components of a boreal forest: Variations during the growing season. *J. Hydrol.* **1997**, *197*, 70–87. [CrossRef]
6. IPCC. Contribution of Working Group I to the Fifth assessment report of the Intergovernmental Panel on Climate Change. In *Climate Change 2013: The Physical Science Basis*; Cambridge University Press: Cambridge, UK; New York, NY, USA, 2013.
7. Gauthier, S.; Bernier, P.; Kuuluvainen, T.; Shvidenko, A.Z.; Schepaschenko, D.G. Boreal forest health and global change. *Science* **2015**, *349*, 819–822. [CrossRef]
8. Astrup, R.; Bernier, P.Y.; Genet, H.; Lutz, D.A.; Bright, R.M. A sensible climate solution for the boreal forest. *Nat. Clim. Chang.* **2018**, *8*, 11–12. [CrossRef]
9. Kang, S.; Kimball, J.S.; Running, S.W. Simulating effects of fire disturbance and climate change on boreal forest productivity and evapotranspiration. *Sci. Total Environ.* **2006**, *362*, 1–3. [CrossRef]
10. Oishi, A.C.; Oren, R.; Novick, K.A.; Palmroth, S.; Katul, G.G. Interannual invariability of forest evapotranspiration and its consequence to water flow downstream. *Ecosystem* **2010**, *13*, 421–436. [CrossRef]
11. Sun, G.; Noormets, A.; Gavazzi, M.J.; McNulty, S.G.; Chen, J.; Domec, J.-C.; King, J.S.; Amatya, D.M.; Skaggs, R.W. Energy and water balance of two contrasting loblolly pine plantations on the lower coastal plain of North Carolina, USA. *For. Ecol. Manag.* **2010**, *259*, 1299–1310. [CrossRef]

12. Staudt, K.; Serafimovich, A.; Siebicke, L.; Pyles, R.D.; Falge, E. Vertical structure of evapotranspiration at a forest site (a case study). *Agric. For. Meteorol.* **2011**, *151*, 709–729. [CrossRef]
13. Bosveld, F.C.; Bouten, W. Evaluating a model of evaporation and transpiration with observations in a partially wet douglas-fir forest. *Bound.-Layer Meteorol.* **2003**, *108*, 365–396. [CrossRef]
14. Savenije, H.H.G. The importance of interception and why we should delete the term evapotranspiration from our vocabulary. *Hydrol. Process.* **2004**, *18*, 1507–1511. [CrossRef]
15. Ge, Z.-M.; Kellomäki, S.; Zhou, X.; Wang, K.-Y.; Peltola, H.; Väisänen, H.; Strandman, H. Effects of climate change on evapotranspiration and soil water availability in Norway spruce forests in southern Finland: An ecosystem model based approach. *Ecohydrology* **2013**, *6*, 51–63. [CrossRef]
16. Wang, L.; Good, S.P.; Caylor, K.K. Global synthesis of vegetation control on evapotranspiration partitioning. *Geophys. Res. Lett.* **2014**, *41*, 6753–6757. [CrossRef]
17. Schlesinger, W.H. and Jasechko, S. Transpiration in the global water cycle. *Agric. For. Meteorol.* **2014**, *189*, 115–117. [CrossRef]
18. Fatichi, S. and Pappas, C. Constrained variability of modeled T:ET ratio across biomes. *Geophys. Res. Lett.* **2017**, *44*, 6795–6803. [CrossRef]
19. Warren, R.K.; Pappas, C.; Helbig, M.; Chasmer, L.E.; Berg, A.A.; Baltzer, J.L.; Quinton, W.L.; Sonnentag, O. Minor contribution of overstorey transpiration to landscape evapotranspiration in boreal permafrost peatlands. *Ecohydrology* **2018**, *11*, 1–10. [CrossRef]
20. Isabelle, P.-E.; Nadeau, D.F.; Anctil, F.; Rousseau, A.N.; Jutras, S.; Music, B. Impacts of high precipitation on the energy and water budgets of a humid boreal forest. *Agric. For. Meteorol.* **2020**, *280*, 107813. [CrossRef]
21. Cienciala, E.; Lindroth, A.; Čermák, J.; Hällgren, J.E.; Kučera, J. Assessment of transpiration estimates for *Picea abies*Picea abies trees during a growing season. *Trees* **1992**, *6*, 121–127. [CrossRef]
22. Aparecido, L.M.T.; Miller, G.R.; Cahill, A.T.; Moore, G.W. Comparison of tree transpiration under wet and dry canopy conditions in a Costa Rican premontane tropical forest. *Hydrol. Process.* **2016**, *30*, 5000–5011. [CrossRef]
23. Granier, A.; Biron, P.; Lemoine, D. Water balance, transpiration and canopy conductance in two beech stands. *Agric. For. Meteorol.* **2000**, *100*, 291–308. [CrossRef]
24. Wilson, K.B.; Hanson, P.J.; Mulholland, P.J.; Baldocchi, D.D.; Wullschleger, S.D. A comparison of methods for determining forest evapotranspiration and its components: Sap-flow, soil water budget, eddy covariance and catchment water balance. *Agric. For. Meteorol.* **2001**, *106*, 153–168. [CrossRef]
25. Giambelluca, T.W, Ziegler, A.D.; Nullet, M.A.; Truong, D.M.; Tran, L.T. Transpiration in a small tropical forest patch. *Agric. For. Meteorol.* **2003**, *117*, 1–22. [CrossRef]
26. Barbour, M.M.; Hunt, J.E.; Walcroft, A.S.; Rogers, G.N.D.; McSeveny, T.M.; Whitehead, D. Components of ecosystem evaporation in a temperate coniferous rainforest, with canopy transpiration scaled using sapwood density. *New Phytol.* **2005**, *165*, 549–558. [CrossRef]
27. Oren, R.; Phillips, N.; Katul, G.; Ewers, B.E.; Pataki, D.E. Scaling xylem sap flux and soil water balance and calculating variance: A method for partitioning water flux in forests. *Ann. For. Sci.* **1998**, *55*, 191–216. [CrossRef]
28. Lu, P.; Urban, L.; Zhao, P. Granier's thermal dissipation probe (TDP) method for measuring sap flow in trees: Theory and practice. *Acta Bot. Sin.* **2004**, *46*, 631–646.
29. Oishi, A.C.; Oren, R.; Stoy, P. C. Estimating components of forest evapotranspiration: A footprint approach for scaling sap flux measurements. *Agric. For. Meteorol.* **2008**, *148*, 1719–1732. [CrossRef]
30. Kumagai, T.; Aoki, S.; Nagasawa, H.; Mabuchi, T.; Kubota, K.; Inoue, S.; Utsumi, Y.; Otsuki, K. Effects of tree-to-tree and radial variations on sap flow estimates of transpiration in Japanese cedar. *Agric. For. Meteorol.* **2005**, *135*, 110–116. [CrossRef]
31. Steppe, K.; De Pauw, D.J.W.; Doody, T.M.; Teskey, R.O. A comparison of sap flux density using thermal dissipation, heat pulse velocity and heat field deformation methods. *Agric. For. Meteorol.* **2010**, *150*, 1046–1056. [CrossRef]
32. Kallarackal, J.; Otieno, D.O.; Reineking, B.; Jung, E.-Y.; Schmidt, M.W.T.; Granier, A.; Tenhunen, J.D. Functional convergence in water use of trees from different geographical regions: A meta-analysis. *Trees* **2013**, *27*, 787–799. [CrossRef]
33. Granier, A. Une nouvelle méthode pour la mesure du flux de sève brute dans le tronc des arbres. *Ann. For. Sci.* **1985**, *42*, 193–200. [CrossRef]

34. Granier, A. Mesure du flux de sève brute dans le tronc du Douglas par une nouvelle méthode thermique. *Ann. For. Sci.* **1987**, *44*, 1–14. [CrossRef]
35. Poyatos, R.; Granda, V.; Molowny-Horas, R.; Mencuccini, M.; Steppe, K.; Martínez-Vilalta, J. SAPFLUXNET: Towards a global database of sap flow measurements. *Tree Physiol.* **2016**, *36*, 1449–1455. [CrossRef]
36. Peters, R.L.; Fonti, P.; Frank, D.C.; Poyatos, R.; Pappas, C.; Kahmen, A.; Carraro, V.; Prendin, A.L.; Schneider, L.; Baltzer, J.L.; et al. Quantification of uncertainties in conifer sap flow measured with the thermal dissipation method. *New Phytol.* **2018**, *219*, 1283–1299. [CrossRef] [PubMed]
37. Bush, S.E.; Hultine, K.R.; Sperry, J.S.; Ehleringer, J.R. Calibration of thermal dissipation sap flow probes for ring- and diffuse-porous trees. *Tree Physiol.* **2010**, *30*, 1545–1554. [CrossRef]
38. Sun, H.; Aubrey, D.P.; Teskey, R.O. A simple calibration improved the accuracy of the thermal dissipation technique for sap flow measurements in juvenile trees of six species. *Trees* **2012**, *26*, 631–640. [CrossRef]
39. Bosch, D.D.; Marshall, L.K.; Teskey, R.O. Forest transpiration from sap flux density measurements in a Southeastern Coastal Plain riparian buffer system. *Agric. For. Meteorol.* **2014**, *187*, 72–82. [CrossRef]
40. Clearwater, M.J.; Meinzer, F.C.; Andrade, J.L.; Goldstein, G.; Holbrook, N.M. Potential errors in measurement of nonuniform sap flow using heat dissipation probes. *Tree Physiol.* **1999**, *19*, 681–687. [CrossRef]
41. Nadezhdina, N.; Čermák, J.; Ceulemans, R. Radial patterns of sap flow in woody stems of dominant and understory species: Scaling errors associated with positioning of sensors. *Tree Physiol.* **2002**, *22*, 907–918. [CrossRef]
42. Fiora, A. and Cescatti, A. Diurnal and seasonal variability in radial distribution of sap flux density: Implications for estimating stand transpiration. *Tree Physiol.* **2006**, *26*, 1217–1225. [CrossRef] [PubMed]
43. Saveyn, A.; Steppe, K.; Lemeur, R. Spatial variability of xylem sap flow in mature beech (*Fagus sylvatica*) and its diurnal dynamics in relation to microclimate. *Botany* **2008**, *86*, 1440–1448. [CrossRef]
44. Rabbel, I.; Diekkrüger, B.; Voigt, H.; Neuwirth, B. Comparing ΔT_{max} determination approaches for Granier-based sapflow estimations. *Sensors* **2016**, *16*, 1–16. [CrossRef]
45. Čermák, J.; Kučera, J.; Nadezhdina, N. Sap flow measurements with some thermodynamic methods, flow integration within trees and scaling up from sample trees to entire forest stands. *Trees* **2004**, *18*, 529–546. [CrossRef]
46. Kool, D.; Agam, N.; Lazarovitch, N.; Heitman, J.L.; Sauer, T.J.; Ben-Gal, A. A review of approaches for evapotranspiration partitioning. *Agric. For. Meteorol.* **2004**, *184*, 56–70. [CrossRef]
47. Wang, S.; Pan, M.; Mu, Q.; Shi, X.; Mao, J.; Brümmer, C.; Jassal, R.S.; Krishnan, P.; Li, J.; Black, T.A. Comparing evapotranspiration from eddy covariance measurements, water budgets, remote sensing, and land surface models over Canada. *J. Hydrometeorol.* **2015**, *16*, 1540–1560. [CrossRef]
48. Soubie, R.; Heinesch, B.; Granier, A.; Aubinet, M.; Vincke, C. Evapotranspiration assessment of a mixed temperate forest by four methods: Eddy covariance, soil water budget, analytical and model. *Agric. For. Meteorol.* **2016**, *228*, 191–204. [CrossRef]
49. Hogg, E.H.; Black, T.A.; den Hartog, G.; Neumann, H.H.; Zimmermann, R.; Hurdle, P.A.; Blanken, P.D.; Nesic, Z.; Yang, P.C.; Staebler, R.M.; et al. A comparison of sap flow and eddy fluxes of water vapor from a boreal deciduous forest. *J. Geophys. Res.: Atmos.* **1997**, *102*, 28929–28937. [CrossRef]
50. Williams, D.G.; Cable, W.; Hultine, K.; Hoedjes, J.C.B.; Yepez, E.A.; Simonneaux, V.; Er-Raki, S.; Boulet, G.; De Bruin, H.A.R.; Chehbouni, A.; Hartogensis, O.K.; Timouk, F. Evapotranspiration components determined by stable isotope, sap flow and eddy covariance techniques. *Agric. For. Meteorol.* **2004**, *125*, 241–258. [CrossRef]
51. Guillemette, F.; Plamondon, A.P.; Prévost, M.; Lévesque, D. Rainfall generated stormflow response to clearcutting a boreal forest: Peak flow comparison with 50 world-wide basin studies. *J. Hydrol.* **2005**, *302*, 137–153. [CrossRef]
52. Senez-Gagnon, F.; Thiffault, E.; Paré, D.; Achim, A.; Bergeron, Y. Dynamics of detrital carbon pools following harvesting of a humid eastern Canadian balsam fir boreal forest. *For. Ecol. Manag.* **2018**, *430*, 33–42. [CrossRef]
53. Tremblay, Y.; Rousseau, A.N.; Plamondon, A.P.; Lévesque, D.; Jutras, S. Rainfall peak flow response to clearcutting 50% of three small watersheds in a boreal forest, Montmorency Forest, Québec. *J. Hydrol.* **2008**, *352*, 67–76. [CrossRef]
54. Tremblay, Y.; Rousseau, A.N.; Plamondon, A.P.; Lévesque, D.; Prévost, M. Changes in stream water quality due to logging of the boreal forest in the Montmorency Forest, Québec. *Hydrol. Process.* **2009**, *23*, 764–776. [CrossRef]

55. Lavigne, M.-P. *Modélisation du Régime Hydrologique et de l'impact des Coupes Forestières sur l'écoulement du Ruisseau des Eaux-Volées à l'aide d'HYDROTEL*. Master Thesis, Institut National de la Recherche Scientifique - Centre Eau Terre Environnement, Québec, QC, Canada, 2007.
56. Noël, P.; Rousseau, A.N.; Paniconi, C.; Nadeau, D.F. Algorithm for delineating and extracting hillslopes and hillslope width functions from gridded elevation data. *J. Hydrol. Eng.* **2013**, *19*, 366–374. [CrossRef]
57. Coyea, M.R.; Margolis, H.A.; Gagnon, R.R. A method for reconstructing the development of the sapwood area of balsam fir. *Tree Physiol.* **1990**, *6*, 283–291. [CrossRef] [PubMed]
58. MELCC. *Données du Programme de Surveillance du Climat*. Direction générale de la surveillance du climat, Ministère de l'Environnement et de la Lutte contre les Changements Climatiques, Québec, QC, Canada, 2019.
59. Wilczak, J.M.; Oncley, S.P.; Stage, S.A. Sonic anemometer tilt correction algorithms. *Bound.-Layer Meteorol.* **2001**, *99*, 127-150. [CrossRef]
60. Reichstein, M.; Falge, E.; Baldocchi, D.; Papale, D.; Aubinet, M.; Berbigier, P.; Bernhofer, C.; Buchmann, N.; Gilmanov, T.; Granier, A.; et al. On the separation of net ecosystem exchange into assimilation and ecosystem respiration: Review and improved algorithm. *Global Change Biol.* **2005**, *11*, 1424–1439. [CrossRef]
61. Dynamax, Inc. *TDP Thermal Dissipation Probe User Manual*; Dynamax, Inc.: Houston, TX, USA, 1997.
62. Delzon, S.; Sartore, M.; Granier, A.; Loustau, D. Radial profiles of sap flow with increasing tree size in maritime pine. *Tree Physiol.* **2004**, *24*, 1285–1293. [CrossRef] [PubMed]
63. Lundblad, M.; Lagergren, F.; Lindroth, A. Evaluation of heat balance and heat dissipation methods for sapflow measurements in pine and spruce. *Ann. For. Sci.* **2001**, *58*, 625–638. [CrossRef]
64. Köstner, B. Evaporation and transpiration from forests in Central Europe–relevance of patch-level studies for spatial scaling. *Meteorol. Atmos. Phys.* **2001**, *76*, 69–82. [CrossRef]
65. METER group, Inc. *PHYTOS 31 Manual*; METER group, Inc.: Pullman, WA, USA, 2018.
66. Pons, T.L.; Jordi, W.; Kuiper, D. Acclimation of plants to light gradients in leaf canopies: Evidence for a possible role for cytokinins transported in the transpiration stream. *J. Exp. Bot.* **2001**, *52*, 1563–1574. [CrossRef] [PubMed]
67. Cohen, Y.; Cohen, S.; Cantuarias-Aviles, T.; Schiller, G. Variations in the radial gradient of sap velocity in trunks of forest and fruit trees. *Plant Soil* **2008**, *305*, 49–59. [CrossRef]
68. Sato, T.; Oda, T.; Igarashi, Y.; Suzuki, M.; Uchiyama, Y. Circumferential sap flow variation in the trunks of Japanese cedar and cypress trees growing on a steep slope. *Hydrol. Res. Lett.* **2012**, *6*, 104–108. [CrossRef]
69. Komatsu, H.; Shinohara, Y.; Kume, T.; Tsuruta, K.; Otsuki, K. Does measuring azimuthal variations in sap flux lead to more reliable stand transpiration estimates? *Hydrol. Process.* **2016**, *30*, 2129–2137. [CrossRef]
70. Loustau, D.; Domec, J.C.; Bosc, A. Interpreting the variations in xylem sap flux density within the trunk of maritime pine (*Pinus pinaster* Ait.): Application of a model for calculating water flows at tree and stand levels. *Ann. For. Sci.* **1998**, *55*, 29–46. [CrossRef]
71. Hacke, U.G.; Lachenbruch, B.; Pittermann, J.; Mayr, S.; Domec, J.C.; Schulte, P.J. The hydraulic architecture of conifers. In *Functional and Ecological Xylem Anatomy*; Hacke, U.G., Eds.; Springer: Cham, Switzerland, 2015.
72. Shinohara, Y.; Tsuruta, K.; Ogura, A.; Noto, F.; Komatsu, H.; Otsuki, K.; Maruyama, T. Azimuthal and radial variations in sap flux density and effects on stand-scale transpiration estimates in a Japanese cedar forest. *Tree Physiol.* **2013**, *33*, 550–558. [CrossRef]
73. Moon, M.; Kim, T.; Park, J.; Cho, S.; Ryu, D.; Suh, S.; Kim, H.S. Changes in spatial variations of sap flow in Korean pine trees due to environmental factors and their effects on estimates of stand transpiration. *J. Mount. Sci.* **2016**, *13*, 1024–1034. [CrossRef]
74. Ford, C.R.; Hubbard, R.M.; Kloeppel, B.D.; Vose, J.M. A comparison of sap flux-based evapotranspiration estimates with catchment-scale water balance. *Agric. For. Meteorol.* **2007**, *145*, 176–185. [CrossRef]
75. O'Brien, J.J.; Oberbauer, S.F.; Clark, D.B. Whole tree xylem sap flow responses to multiple environmental variables in a wet tropical forest. *Plant Cell Environ.* **2004**, *27*, 551–567. [CrossRef]
76. Kume, T.; Kuraji, K.; Yoshifuji, N.; Morooka, T.; Sawano, S.; Chong, L.; Suzuki, M. Estimation of canopy drying time after rainfall using sap flow measurements in an emergent tree in a lowland mixed-dipterocarp forest in Sarawak, Malaysia. *Hydrol. Process.* **2006**, *20*, 565–578. [CrossRef]
77. Rutter, A.J.; Kershaw, K.A.; Robins, P.C.; Morton, A.J. A predictive model of rainfall interception in forests, 1. Derivation of the model from observations in a plantation of Corsican pine. *Agric. Meteorol.* **1971**, *9*, 367–384. [CrossRef]

78. Saugier, B.; Granier, A.; Pontailler, J.Y.; Dufrene, E.; Baldocchi, D.D. Transpiration of a boreal pine forest measured by branch bag, sap flow and micrometeorological methods. *Tree Physiol.* **1997**, *17*, 511–519. [CrossRef] [PubMed]
79. Tyree, M.T. Hydraulic limits on tree performance: Transpiration, carbon gain and growth of trees. *Trees* **2003**, *17*, 95–100. [CrossRef]
80. Bréda, N.; Granier, A.; Aussenac, G. Effects of thinning on soil and tree water relations, transpiration and growth in an oak forest (*Quercus petraea* (Matt.) Liebl. *Tree Physiol.* **1995**, *15*, 295–306. [CrossRef] [PubMed]
81. Granier, A.; Loustau, D.; Bréda, N. A generic model of forest canopy conductance dependent on climate, soil water availability and leaf area index. *Ann. For. Sci.* **2000**, *57*, 755–765. [CrossRef]
82. Gigante, V.; Iacobellis, V.; Manfreda, S.; Milella, P.; Portoghese, I. Influences of Leaf Area Index estimations on water balance modeling in a Mediterranean semi-arid basin. *Nat. Hazards Earth Syst. Sci.* **2009**, *9*, 979–991. [CrossRef]
83. Simic, A.; Fernandes, R.; Wang, S. Assessing the impact of leaf area index on evapotranspiration and groundwater recharge across a shallow water region for diverse land cover and soil properties. *J. Water Resour. Hydraul. Eng.* **2014**, *3*, 60–73.
84. Tesemma, Z.K.; Wei, Y.; Peel, M.C.; Western, A.W. Including the dynamic relationship between climatic variables and leaf area index in a hydrological model to improve streamflow prediction under a changing climate. *Hydrol. Earth Syst. Sci.* **2015**, *19*, 2821–2836. [CrossRef]
85. Isabelle, P.-E.; Nadeau, D.F.; Asselin, M.H.; Harvey, R.; Musselman, K.N.; Rousseau, A.N.; Anctil, F. Solar radiation transmittance of a boreal balsam fir canopy: Spatiotemporal variability and impacts on growing season hydrology. *Agric. For. Meteorol.* **2018**, *263*, 1–14. [CrossRef]
86. Shimizu, T.; Kumagai, T.O.; Kobayashi, M.; Tamai, K.; Iida, S.I.; Kabeya, N.; Ikawa, R.; Tateishi, M.; Miyazawa, Y.; Shimizu, A. Estimation of annual forest evapotranspiration from a coniferous plantation watershed in Japan (2): Comparison of eddy covariance, water budget and sap-flow plus interception loss. *J. Hydrol.* **2015**, *522*, 250–264. [CrossRef]
87. Paul-Limoges, E.; Wolf, S.; Schneider, F.D.; Longo, M.; Moorcroft, P.; Gharun, M.; Damm, A. Partitioning evapotranspiration with concurrent eddy covariance measurements in a mixed forest. *Agric. For. Meteorol.* **2020**, *280*, 107786. [CrossRef]
88. Kozii, N.; Haahti, K.; Tor-ngern, P.; Chi, J.; Hasselquist, E.M.; Laudon, H.; Launiainen, S.; Oren, R.; Peichi, M.; Wallerman, J.; et al. Partitioning the forest water balance within a boreal catchment using sapflux, eddy covariance and process-based model. *Hydrol. Earth Syst. Sci. Discuss.* **2019**, *2019*, 1–50.